

The strange and light quark contributions to the nucleon mass from Lattice QCD

Gunnar S. Bali,^{1,*} Sara Collins,^{1,†} Meinulf Gökeler,¹ Roger Horsley,² Yoshifumi Nakamura,³ Andrea Nobile,¹ Dirk Pleiter,^{4,1} P.E.L. Rakow,⁵ Andreas Schäfer,¹ Gerrit Schierholz,⁶ André Sternbeck,¹ and James M. Zanotti^{7,2}

(QCDSF Collaboration)

¹*Institut für Theoretische Physik, Universität Regensburg, 93040 Regensburg, Germany*

²*School of Physics, University of Edinburgh, Edinburgh EH9 3JZ, UK*

³*RIKEN Advanced Institute for Computational Science, Kobe, Hyogo 650-0047, Japan*

⁴*JSC, Research Center Jülich, 52425 Jülich, Germany*

⁵*Theoretical Physics Division, Department of Mathematical Sciences, University of Liverpool, Liverpool L69 3BX, UK*

⁶*Deutsches Elektronen-Synchrotron DESY, 22603 Hamburg, Germany*

⁷*Special Research Centre for the Subatomic Structure of Matter, School of Chemistry & Physics, University of Adelaide, South Australia 5005, Australia*

(Dated: September 13, 2018)

We determine the strangeness and light quark fractions of the nucleon mass by computing the quark line connected and disconnected contributions to the matrix elements $m_q \langle N | \bar{q}q | N \rangle$ in lattice QCD, using the non-perturbatively improved Sheikholeslami-Wohlert Wilson Fermionic action. We simulate $n_F = 2$ mass degenerate sea quarks with a pion mass of about 285 MeV and a lattice spacing $a \approx 0.073$ fm. The renormalization of the matrix elements involves mixing between contributions from different quark flavours. The pion-nucleon σ -term is extrapolated to physical quark masses exploiting the sea quark mass dependence of the nucleon mass. We obtain the renormalized values $\sigma_{\pi N} = (38 \pm 12)$ MeV at the physical point and $f_{T_s} = \sigma_s/m_N = 0.012(14)_{-3}^{+10}$ for the strangeness contribution at our larger than physical sea quark mass.

PACS numbers: 12.38.Gc, 13.85.-t, 14.20.Dh

I. INTRODUCTION

Most of the nucleon's mass is generated by the spontaneous breaking of chiral symmetry and only a small part can be attributed directly to the masses of its valence and sea quarks. The quantities

$$f_{T_q} = m_q \langle N | \bar{q}q | N \rangle / m_N \quad (1)$$

parameterize the fractions of the nucleon mass m_N that are carried by quarks of flavour q . Almost all visible matter of the universe is composed of nucleons and yet little is known experimentally about these quark contributions to their mass.

The scalar matrix elements

$$\sigma_q = m_q \langle N | \bar{q}q | N \rangle = m_N f_{T_q} \quad (2)$$

also determine the coupling strength of the Standard Model (SM) Higgs boson (or of any similar scalar particle) at zero recoil to the nucleon. This then might couple to heavy particles that could be discovered in LHC experiments, some of which are dark matter candidates [1]. The combination $m_N \sum_q f_{T_q}$, $q \in \{u, d, s\}$, will appear quadratically in this cross section that is proportional to $|f_N|^2$ where

$$\frac{f_N}{m_N} = \sum_{q \in \{u, d, s\}} f_{T_q} \frac{\alpha_q}{m_q} + \frac{2}{27} f_{T_G} \sum_{q \in \{c, b, t\}} \frac{\alpha_q}{m_q}, \quad (3)$$

with the couplings $\alpha_q \propto m_q/m_W$. Due to the trace anomaly of the energy momentum tensor one obtains [2]

$$f_{T_G} = 1 - \sum_{q \in \{u, d, s\}} f_{T_q}. \quad (4)$$

Note that the coupling f_N of Eq. (3) only mildly depends on the masses of heavy quark flavours [2, 3].

The σ_q -terms are also needed for precision measurements of SM parameters in pp collisions at the LHC. For instance the resolution of a (hypothetical) mass difference between the W^+ and W^- bosons is limited by our knowledge of the asymmetries between the up and down as well as between the strange and charm sea quark contents of the proton [4]. An accurate calculation of these quantities will help to increase the precision of SM phenomenology and to shed light on non-SM processes.

The light quark contribution, the pion-nucleon σ -term, is defined as

$$\begin{aligned} \sigma_{\pi N} &= \sigma_u + \sigma_d = m_u \frac{\partial m_N}{\partial m_u} + m_d \frac{\partial m_N}{\partial m_d} \\ &\approx m_{PS}^2 \left. \frac{dm_N}{dm_{PS}^2} \right|_{m_{PS}=m_\pi}, \end{aligned} \quad (5)$$

where m_{PS} denotes the pseudoscalar mass. Some time ago, employing dispersive analyses of pion-nucleon scattering data, the values [5] $\sigma_{\pi N} = 45(8)$ MeV and [6] $\sigma_{\pi N} = 64(7)$ MeV were obtained while a calculation in the framework of $\mathcal{O}(p^4)$ heavy baryon chiral perturbation theory resulted in [7] $\sigma_{\pi N} = 48(10)$ MeV. A recent covariant baryon chiral perturbation theory (B χ PT) analysis

* gunnar.bali@ur.de

† sara.collins@physik.uni-regensburg.de

of the available pion-nucleon scattering data [8] resulted in the value $\sigma_{\pi N} = 59(7)$ MeV. Even less is known about the strangeness contribution σ_s . Since no elastic Higgs-nucleon scattering experiments exist all phenomenological estimates largely depend on modelling. Therefore input from lattice simulations is urgently required.

We have witnessed an upsurge of interest in calculating flavour singlet matrix elements recently, either directly [9–13], by calculating the corresponding quark line connected and disconnected terms, or indirectly, via the Feynman-Hellmann theorem [13–19]. High statistics simulations including light sea quarks mean that reasonable signals can be obtained for disconnected terms. Similarly, the small statistical uncertainty on baryon masses as functions of the quark masses enable reasonable fits to be made. Ideally, the results of both approaches should agree.

Preliminary results of this study were presented at past Lattice conferences [20, 21]. This article is organised as follows. In Sec. II we detail the gauge configurations, simulation parameters and methods used. In Sec. III we then explain how the lattice results are renormalized and finally we present our results in Sec. IV, before we summarize.

II. SIMULATION DETAILS AND METHODS

We simulate $n_F = 2$ non-perturbatively improved Sheikholeslami-Wohlert fermions, using the Wilson gauge action, at $\beta = 5.29$ and $\kappa = \kappa_{ud} = 0.13632$. Setting the scale from the chirally extrapolated nucleon mass, we obtain [22] the value $r_0 = 0.508(13)$ fm for the Sommer scale, in the physical limit. This results in the lattice spacing

$$a^{-1} = (6.983 \pm 0.049) r_0^{-1} = (2.71 \pm 0.02 \pm 0.07) \text{ GeV}, \quad (6)$$

where the errors are statistical and from the scale setting, respectively. The r_0/a ratio is obtained by chirally extrapolating the QCDSF $\beta = 5.29$ simulation points [23]. An extrapolation of the axial Takahashi-Ward identity (AWI) mass yields the critical hopping parameter value

$$\kappa_{c, \text{sea}} = 0.1364396(84). \quad (7)$$

In addition to $\kappa_{ud} = \kappa_{\text{sea}} = 0.13632$, we realize the valence κ -values, $\kappa_m = 0.13609$ and $\kappa_s = 0.13550$. The corresponding three pseudoscalar masses read

$$m_{\text{PS}, ud} = (0.1050 \pm 0.0003) a^{-1} = (285 \pm 3 \pm 7) \text{ MeV}, \quad (8)$$

$$m_{\text{PS}, m} = (449 \pm 3 \pm 11) \text{ MeV}, \quad (9)$$

$$m_{\text{PS}, s} = (720 \pm 5 \pm 18) \text{ MeV}. \quad (10)$$

The strange quark mass was fixed so that the above value for $m_{\text{PS}, s}$ is close to the mass of a hypothetical strange-antistrange pseudoscalar meson: $(m_{K^\pm}^2 + m_{K^0}^2 -$

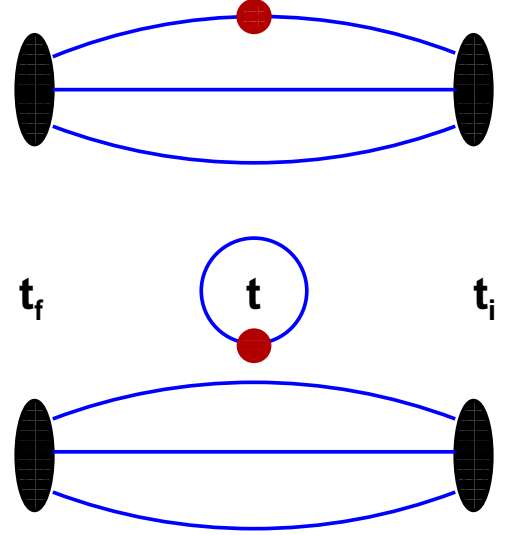


FIG. 1. Quark line connected (top) and disconnected (bottom) three-point functions. We have omitted the relative minus sign between the diagrams. Note that for scalar matrix elements, the vacuum expectation value of the current insertion needs to be subtracted ($\bar{q}q \mapsto \bar{q}q - \langle \bar{q}q \rangle$), see Eq. (12).

$m_{\pi^\pm}^2)^{1/2} \approx 686.9$ MeV. We investigate volumes of $32^3 64$ and $40^3 64$ lattice points, i.e., $L m_{\text{PS}} = 3.36$ and 4.20 , respectively, where the largest spatial lattice extent is $L \approx 2.91$ fm. We analyse 2024 thermalized trajectories on each of the volumes. To effectively eliminate auto-correlations for the observables that we are interested in, bin sizes of eight are found to be sufficient.

The matrix element $\langle N | \bar{q}q | N \rangle$ is extracted from the ratio of three-point functions, see Fig. 1, to two-point functions at zero momentum. Defining

$$\text{Tr}_t A = \sum_{\mathbf{x}} \text{Tr} A(\mathbf{x}, t; \mathbf{x}, t), \quad (11)$$

we can write the disconnected part as

$$R^{\text{dis}}(t_f, t) = \langle \text{Tr}_t(M^{-1} \mathbb{1}) \rangle - \frac{\langle C_{2\text{pt}}(t_f) \text{Tr}_t(M^{-1} \mathbb{1}) \rangle}{\langle C_{2\text{pt}}(t_f) \rangle}, \quad (12)$$

where M is the lattice Dirac operator for the quark flavour q of the current and $C_{2\text{pt}}(t_f)$ denotes the two-point function of the zero momentum projected proton connecting the source time $t_i = 0$ with t_f . Note that, unlike its expectation value, $C_{2\text{pt}}$ computed on one configuration will in general also have an imaginary part. This means that we can reduce the variance of the above expression by explicitly setting this to zero, using the relation $\text{Im} \text{Tr}_t(M^{-1} \mathbb{1}) = 0$ that follows from the γ_5 -Hermiticity, $M^\dagger = \gamma_5 M \gamma_5$.

In the limit of large times, $t_f \gg t \gg 0$,

$$R^{\text{dis}}(t_f, t) + R^{\text{con}}(t_f, t) \longrightarrow \langle N | \bar{q}q | N \rangle, \quad (13)$$

where the term $R^{\text{con}}(t_f, t) = C_{3\text{pt}}(t_f, t)/C_{2\text{pt}}(t_f)$ only contributes for $q \in \{u, d\}$. Quark field smearing (see below)

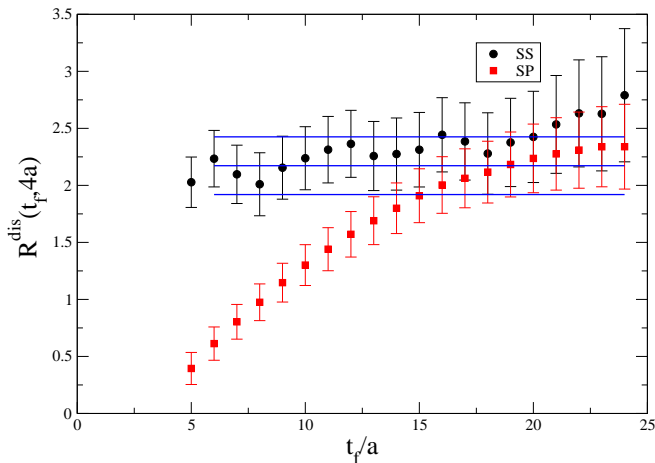


FIG. 2. Dependence of R^{dis} on t_f for smeared-smeared (SS) and smeared-point (SP) two-point functions, together with the fit result.

at the source and the sink significantly enhances the coupling of the nucleon creation and destruction operators to the physical ground state. Still, the time distances between the source and the current insertion t as well as between the current and the sink $t_f - t$ need to be taken sufficiently large to suppress excited state contributions.

We find the nucleon smeared-smeared effective masses to be constant for $t \geq 8a$. It suffices if excited state effects are much smaller than the statistical errors. These errors however are expected to be substantially larger for the disconnected three-point function than for the nucleon two-point function. Thus, we set the time of the current insertion to a smaller value $t = 4a \approx 0.29$ fm. The method that we apply requires us to fix t , but t_f can be varied. If the R^{dis} data were not constant for $t_f \geq 2t = 8a$ then this would have implied that our choice of t was too ambitious. Fortunately, employing sink and source smearing, we find the asymptotic limit to be effectively reached for $t_f \geq 5a$ and compute the matrix elements by fitting the above ratios for $t_f \geq 6a \approx 0.44$ fm to constants.

As an example, in Fig. 2 we display the disconnected ratio for strange valence and current quark masses as a function of t_f for smeared-smeared three- over two-point functions for $40^3 64$ lattices, together with this fit result. In addition we show the corresponding smeared-point ratio that converges towards the same value, giving us additional confidence that t was chosen sufficiently large to warrant ground state dominance within our statistical errors.

Based on Ref. [24] we improve the overlap of our nucleon creation operator with the ground state by applying Wuppertal-smearing [25]

$$\phi_x^{(n)} = \frac{1}{1 + 6\delta} \left(\phi_x^{(n-1)} + \delta \sum_{j=\pm 1}^{\pm 3} U_{x,j} \phi_{x+a\hat{j}}^{(n-1)} \right) \quad (14)$$

to quark fields ϕ , where we set $\delta = 0.25$ and use 400 iterations. We replace the spatial links $U_{x,j}$ above by

APE-smearing [26] links

$$U_{x,i}^{(n)} = P_{\text{SU}(3)} \left(\alpha U_{x,i}^{(n-1)} + \sum_{|j| \neq i} U_{x,j}^{(n-1)} U_{x+a\hat{j},i}^{(n-1)} U_{x+a\hat{i},j}^{(n-1)\dagger} \right), \quad (15)$$

where $i \in \{1, 2, 3\}$, $j \in \{\pm 1, \pm 2, \pm 3\}$. $P_{\text{SU}(3)}$ denotes a projection operator into the $\text{SU}(3)$ group and the sum is over the four spatial “staples”, surrounding $U_{x,i}$. We employ 25 such gauge covariant smearing iterations and use the weight factor $\alpha = 2.5$. For the projector we somewhat deviate from Ref. [24] and maximize $\text{Re Tr} [A^\dagger P_{\text{SU}(3)}(A)]$, iterating over $\text{SU}(2)$ subgroups. The connected part, for which the statistical accuracy is less of an issue, is obtained with a less effective smearing at the larger, fixed value $t_f = 15a$, varying t .

We stochastically estimate $\text{Tr}_t M^{-1}$. For this purpose we employ N complex \mathbb{Z}_2 noise vectors, $|\eta^i\rangle_t$, $i = 1, \dots, N$, whose spacetime \otimes spin \otimes colour components $e^{i\phi}$ carry uncorrelated random phases $\phi \in \{\pm\pi/4, \pm 3\pi/4\}$ at the time t and are set to zero elsewhere, to reduce the noise (partitioning [27]).

Solving the linear systems

$$M|s^i\rangle_t = |\eta^i\rangle_t \quad (16)$$

for $|s^i\rangle_t$ we can then substitute,

$$\text{Tr}_t M_E^{-1} = \frac{1}{N} \sum_i \langle \eta^i | s^i \rangle_t = \text{Tr}_t M^{-1} + \mathcal{O} \left(\frac{1}{\sqrt{N}} \right). \quad (17)$$

The inner product is only taken over three-space, spin and colour indices. In the case of the scalar matrix element it is relatively easy to push the stochastic error below the level of the inherent error from fluctuations between gauge configurations¹ [28]. Therefore, here we do not need to employ the Truncated Solver Method (TSM) [28] and do not exploit the hopping parameter expansion. Instead, to reduce the dominant gauge error, we compute the nucleon two-point functions for four equidistant source times on each gauge configuration. In addition we exploit backwardly propagating nucleons, replacing the positive parity projector $\frac{1}{2}(\mathbb{1} + \gamma_4)$ by $\frac{1}{2}(\mathbb{1} - \gamma_4)$ within the nucleon two-point function, $C_{2\text{pt}}$. Consequently, the noise vectors are seeded on 8 time slices simultaneously, reducing the degree of time partitioning. We find this not to have any adverse effect on the stochastic error. In addition to the 48 (4 timeslices times 4 spinor components times 3 colours) point-to-all sources necessary to compute the two-point functions we solve for $N = 50$ noise vectors per configuration and current quark mass.

¹ Note that both error sources will scale in proportion to $1/\sqrt{n_{\text{conf}}}$.

III. RENORMALIZATION

In the continuum, for light quark flavours q , the σ_q -terms are invariant under renormalization group transformations. However, Wilson fermions explicitly break chiral symmetry and this enables mixing not only with gluonic contributions but also with other quark flavours. Note that due to the use of a quenched strange quark, the renormalization of the corresponding matrix element is particularly large and needs to be studied carefully. A consistent $\mathcal{O}(a)$ improvement of the quark scalar matrix elements requires the inclusion of the gluonic operator aGG . We have not measured this as yet. Therefore we will neither include any $\mathcal{O}(a)$ improvement of the renormalization constants nor of the scalar current. However, we will account for the mixing between quark flavours.

We follow the procedure outlined in Ref. [29], see also Sec. 6 of Ref. [30]. The same result can be obtained by taking derivatives of the nucleon mass with respect to the sea quark masses [31] via the Feynman-Hellmann theorem. This also holds for the case of a partially quenched strange quark [9, 15]. In the renormalization the strangeness matrix element will receive subtractions not only from light quark disconnected but also from the numerically larger connected diagrams. This has first been pointed out in Ref. [32].

For Wilson actions the vector Takahashi-Ward identity (VWI) lattice quark mass is given by

$$m_q = \frac{1}{2a} \left(\frac{1}{\kappa_q} - \frac{1}{\kappa_{c, \text{sea}}} \right). \quad (18)$$

In the partially quenched theory one can define a $\kappa_{c, \text{val}}(\beta, \kappa_{\text{sea}}) \neq \kappa_{c, \text{sea}}(\beta)$ as the κ -value at which the valence pseudoscalar mass vanishes.

We distinguish between singlet and non-singlet quark masses that will renormalize differently. In the case of the theory with $n_F = 2 + 1$ ($m_u = m_d = m_{ud}$) sea quarks, we have a mass term

$$\begin{aligned} \mathcal{L}_m &= m_{ud}(\bar{u}u + \bar{d}d) + m_s \bar{s}s \\ &= \bar{m} \bar{\psi} \mathbb{1} \psi + m^{ns} \bar{\psi} \lambda_8 \psi, \end{aligned} \quad (19)$$

$$\bar{m} = \frac{1}{3}(2m_{ud} + m_s), \quad (20)$$

where $\bar{\psi} = (\bar{u}, \bar{d}, \bar{s})$; the lattice singlet quark mass \bar{m} is given by the average of the sea quark masses.

A renormalized quark mass for the flavour q at a scale μ is given by

$$m_q^{\text{ren}}(\mu) = Z_m^s(\mu) \bar{m} + Z_m^{ns}(\mu)(m_q - \bar{m}), \quad (21)$$

where singlet quark masses renormalize with a renormalization constant $Z_m^s(\mu)$ and non-singlet combinations with $Z_m^{ns}(\mu)$. Notice that the ratio Z_m^s/Z_m^{ns} is independent of the scale μ but depends on the lattice spacing a , through the coupling $\alpha_s(a^{-1})$.

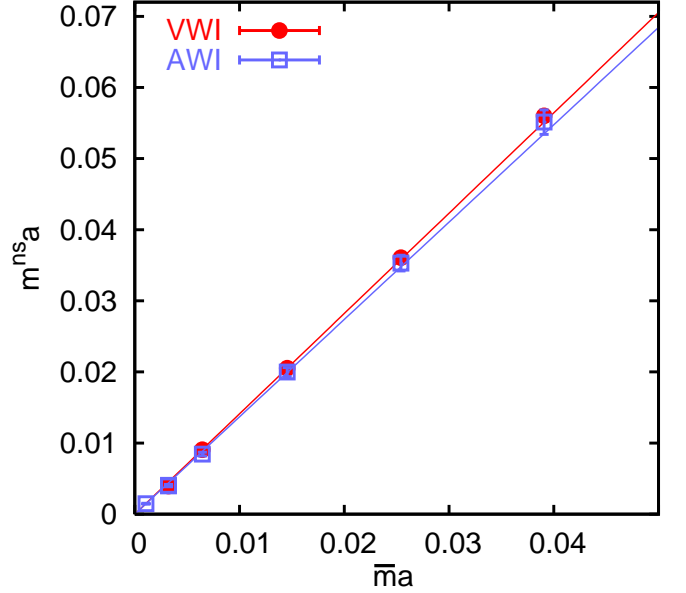


FIG. 3. Determination of the slope $Z_m^s/Z_m^{ns} = 1 + \alpha_Z$, see Eqs. (25) and (27).

In the partially quenched theory with mass degenerate sea quarks Eq. (21) results in

$$\bar{m}^{\text{ren}}(\mu) = Z_m^s(\mu) \bar{m}, \quad (22)$$

$$\bar{m}^{\text{ren}}(\mu) - m^{\text{val, ren}}(\mu) = Z_m^{ns}(\mu)(\bar{m} - m^{\text{val}}), \quad (23)$$

where we introduce a VWI valence quark mass through

$$m^{\text{val}} = \frac{1}{2a} \left(\frac{1}{\kappa_{\text{val}}} - \frac{1}{\kappa_{c, \text{sea}}} \right). \quad (24)$$

At $\kappa_{\text{val}} = \kappa_{c, \text{val}}$, $m^{\text{val, ren}}$ vanishes so that we obtain

$$\begin{aligned} \frac{Z_m^s}{Z_m^{ns}} &= \frac{m^{ns}}{\bar{m}} = \frac{\bar{m} - m^{\text{val}}}{\bar{m}} \Big|_{\kappa_{\text{val}} = \kappa_{c, \text{val}}} \\ &= \frac{\kappa_{\text{sea}}^{-1} - \kappa_{c, \text{val}}^{-1}}{\kappa_{\text{sea}}^{-1} - \kappa_{c, \text{sea}}^{-1}} =: 1 + \alpha_Z. \end{aligned} \quad (25)$$

The non-singlet mass above can also be obtained from the bare AWI mass,

$$m^{ns, \text{ren}} = Z_m^{ns} m^{ns} = \frac{Z_A^{ns}}{Z_P^{ns}} m^{\text{AWI}}, \quad (26)$$

that renormalizes with the ratio of the renormalization constants Z_A^{ns} over Z_P^{ns} of the non-singlet axial and pseudoscalar currents. This results in the alternative prescription to Eq. (25),

$$\frac{Z_m^s}{Z_m^{ns}} = \frac{Z_A^{ns}}{Z_m^{ns} Z_P^{ns}} \frac{2a m^{\text{AWI}}}{\kappa_{\text{sea}}^{-1} - \kappa_{c, \text{sea}}^{-1}}, \quad (27)$$

where m^{AWI} is calculated at κ_{sea} . The required combination of scalar, pseudoscalar and axial non-isosinglet

renormalization factors for our simulation with $n_F = 2$ sea quarks at $\beta = 5.29$ reads [33]

$$Z_A^{ns}/(Z_m^{ns} Z_P^{ns}) = 0.988 \pm 0.031. \quad (28)$$

The two methods that differ by terms of $\mathcal{O}(a)$ are illustrated in Fig. 3 for our configurations with $n_F = 2$ mass degenerate sea quark flavours.

The results read

$$\alpha_Z = \begin{cases} 0.411(13) & , \text{ VWI} \\ 0.369(22) & , \text{ AWI} \end{cases} \quad (29)$$

Corrections to these values at a non-zero quark mass m will be of $\mathcal{O}(ma)$; the differences between the two definitions are indicative of $\mathcal{O}(a)$ effects. We remark that α_Z is of leading order α_s^2 in the strong coupling parameter and it will therefore decrease with the lattice spacing a .

For $n_F = 2 + 1$ sea quarks Eq. (21) amounts to

$$m_q^{\text{ren}}(\mu) = Z_m^{ns}(\mu) m_q + (Z_m^s(\mu) - Z_m^{ns}(\mu)) \overline{m} \quad (30)$$

$$= Z_m^{ns}(\mu) (m_q + \alpha_Z \overline{m}),$$

where α_Z is defined in Eq. (25). This can be written as

$$\begin{pmatrix} m_u(\mu) \\ m_d(\mu) \\ m_s(\mu) \end{pmatrix}^{\text{ren}} = Z_m^{ns}(\mu, a) \begin{pmatrix} 1 + \frac{\alpha_Z(a)}{3} & \frac{\alpha_Z(a)}{3} & \frac{\alpha_Z(a)}{3} \\ \frac{\alpha_Z(a)}{3} & 1 + \frac{\alpha_Z(a)}{3} & \frac{\alpha_Z(a)}{3} \\ \frac{\alpha_Z(a)}{3} & \frac{\alpha_Z(a)}{3} & 1 + \frac{\alpha_Z(a)}{3} \end{pmatrix} \begin{pmatrix} m_u(a) \\ m_d(a) \\ m_s(a) \end{pmatrix}^{\text{lat}}, \quad (31)$$

where the lattice quark masses on the right hand side are defined by the VWI, Eq. (18). For clarity we have included the lattice spacing dependence above, which below we will drop again. The sum $\sum_q m_q^{\text{ren}}(\mu) \langle N | \bar{q}q | N \rangle^{\text{ren}}(\mu)$ is invariant under renormalization group transformations². Therefore the scalar lattice matrix elements will renormalize with the inverse matrix above: the different quark contributions will mix in the mass non-degenerate case.

We now turn to the situation of interest of $n_F = 2$ light sea quarks, with a quenched strange quark. This means that the singlet mass $\overline{m}^{\text{lat}} = (m_u^{\text{lat}} + m_d^{\text{lat}})/2$ will not depend on the strange quark mass anymore. (The superscript “lat” has been added for clarity.) Eq. (30) can now be written as

$$\begin{pmatrix} m_u(\mu) \\ m_d(\mu) \\ m_s(\mu) \end{pmatrix}^{\text{ren}} = Z_m^{ns}(\mu) \begin{pmatrix} 1 + \frac{\alpha_Z}{2} & \frac{\alpha_Z}{2} & 0 \\ \frac{\alpha_Z}{2} & 1 + \frac{\alpha_Z}{2} & 0 \\ \frac{\alpha_Z}{2} & \frac{\alpha_Z}{2} & 1 \end{pmatrix} \begin{pmatrix} m_u \\ m_d \\ m_s \end{pmatrix}^{\text{lat}}, \quad (32)$$

where the presence of the strange quark is not felt by the sea quarks. However, the definition of m_s involves $\kappa_{c,\text{sea}}$. Inverting the above matrix yields³

$$\begin{pmatrix} \langle \bar{u}u \rangle(\mu) \\ \langle \bar{d}d \rangle(\mu) \\ \langle \bar{s}s \rangle(\mu) \end{pmatrix}^{\text{ren}} = \frac{1}{(1 + \alpha_Z) Z_m^{ns}(\mu)} \begin{pmatrix} 1 + \frac{\alpha_Z}{2} & -\frac{\alpha_Z}{2} & 0 \\ -\frac{\alpha_Z}{2} & 1 + \frac{\alpha_Z}{2} & 0 \\ -\frac{\alpha_Z}{2} & -\frac{\alpha_Z}{2} & 1 + \alpha_Z \end{pmatrix} \begin{pmatrix} \langle \bar{u}u \rangle \\ \langle \bar{d}d \rangle \\ \langle \bar{s}s \rangle \end{pmatrix}^{\text{lat}}. \quad (33)$$

For the light quark matrix element (i.e. the $\sigma_{\pi N}$ -term) this means that

$$\frac{m_u^{\text{ren}}(\mu) + m_d^{\text{ren}}(\mu)}{2} \langle N | \bar{u}u + \bar{d}d | N \rangle^{\text{ren}}(\mu) = \frac{m_u^{\text{lat}} + m_d^{\text{lat}}}{2} \langle N | \bar{u}u + \bar{d}d | N \rangle^{\text{lat}}, \quad (34)$$

while for the strangeness matrix element we obtain

$$[m_s \langle N | \bar{s}s | N \rangle]^{\text{ren}} = \left[m_s^{\text{lat}} + \frac{\alpha_Z}{2} (m_u^{\text{lat}} + m_d^{\text{lat}}) \right] \left(\langle N | \bar{s}s | N \rangle^{\text{lat}} - \frac{\alpha_Z}{2(1 + \alpha_Z)} \langle N | \bar{u}u + \bar{d}d | N \rangle^{\text{lat}} \right). \quad (35)$$

² Note that these scalar matrix elements are differences of scalar currents $\bar{q}q$ within the nucleon, relative to their vacuum expectation values. Therefore, unlike the chiral condensates alone, they do not undergo any additive renormalization and do not mix with an $a^{-3}\mathbb{1}$ term.

³ Here and occasionally below we omit specifying the external state (in our case $|N\rangle$) in cases where identities between hadronic matrix elements are independent of this state.

Again, the lattice strange quark mass is defined as $m_s^{\text{lat}} = (\kappa_s^{-1} - \kappa_{c,\text{sea}}^{-1})/(2a)$. The same renormalization pattern can also be derived, employing the Feynman-Hellmann theorem [9, 15].

It is evident from Eq. (33) that the so-called y -ratio

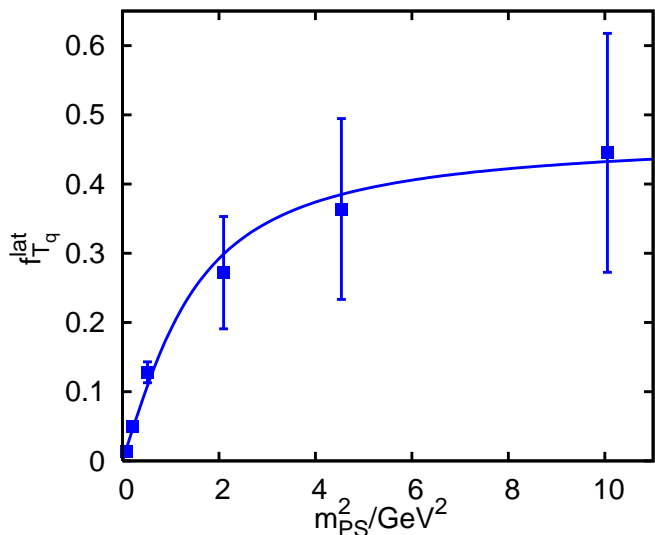


FIG. 4. The unrenormalized mass fraction $f_{T_q}^{\text{lat}}$, as a function of the current pseudoscalar mass on the $L = 32a$ lattices, at the smallest valence mass $m_{\text{PS}} \approx 285$ MeV.

renormalizes as follows,

$$y := \frac{2\langle N|\bar{s}s|N\rangle^{\text{ren}}}{\langle N|\bar{u}u + \bar{d}d|N\rangle^{\text{ren}}} = (1 + \alpha_Z) \frac{2\langle N|\bar{s}s|N\rangle^{\text{lat}}}{\langle N|\bar{u}u + \bar{d}d|N\rangle^{\text{lat}}} - \alpha_Z. \quad (36)$$

IV. RESULTS

As discussed in Sec. II above we employ three hopping parameter values, $\kappa_{ud} = \kappa_{\text{sea}} = 0.13632$, $\kappa_m = 0.13609$ and $\kappa_s = 0.13550$, that correspond to the pseudoscalar masses $m_{\text{PS}} \approx 285$ MeV, 450 MeV and 720 MeV, respectively, see Eqs. (8) – (10). We use all these κ -values for the valence quarks (κ_{val}) as well as for the current insertions $\bar{q}q$ (κ_{cur}). This amounts to nine combinations for the disconnected ratios R^{dis} while for the connected part $\kappa_{\text{cur}} = \kappa_{\text{val}}$.

We will explore the dependence of the lattice matrix elements on the current quark mass and investigate finite size effects, using a partial summation method. Subsequently, unrenormalized and renormalized valence and sea quark contributions are studied. Finally, we compute the light σ -term, the mass contributions f_{T_s} and f_{T_G} and the y -ratio.

A. Dependence of the lattice matrix elements on the current quark mass

From the heavy quark expansion it is evident that $f_{T_q} \propto \langle N|GG|N\rangle/m_N \propto f_{T_G}$ for $m_q \rightarrow \infty$. This can also be seen on the lattice where the leading non-vanishing

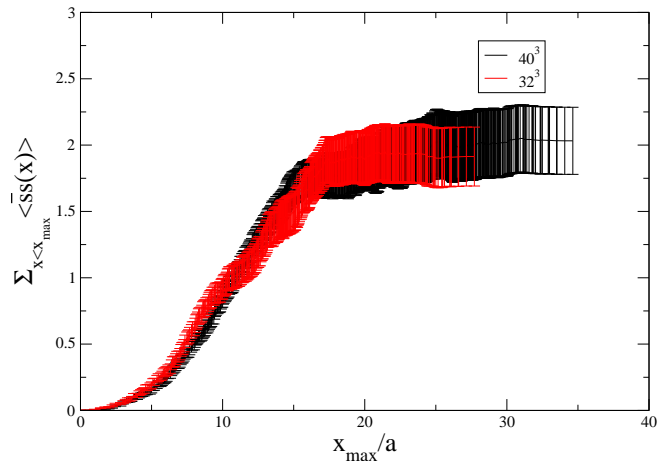


FIG. 5. Eq. (12), partially summed up to a maximum spatial distance from the source x_{max} , see Eq. (37).

contribution in the hopping parameter expansion is proportional to the plaquette. To confirm this expected saturation we compute the scalar matrix element for three additional current quark masses up to and above the charm quark mass m_c on a subset of 576 $32^3 64$ lattices, using our smallest valence quark mass. We remark that for an $\mathcal{O}(a)$ improvement of the operator $\bar{q}q$, mixing with aGG needs to be considered. These improvement terms will become large if $m_q a$ is big. In fact the renormalized f_{T_q} becomes negative at about twice the strange quark mass if we neglect such effects. We have not investigated gluonic contributions as yet and therefore the behaviour at large masses is beyond the scope of the present study. For very small quark masses we would expect $f_{T_q} \propto m_q$. Indeed, these expectations are confirmed for the unrenormalized $f_{T_q}^{\text{lat}}$, as can be seen in Fig. 4. Note that the third data point from the left corresponds to the strange quark mass while the charm quark can be found at the value $m_{\text{PS}}^2 \approx 8.9$ GeV². The arctan-curve is drawn to guide the eye.

B. Finite size effects: partial sums

In order to investigate finite size effects we find it worthwhile to replace the numerator of Eq. (12) by a partial sum:

$$- \sum_{|\mathbf{x}| \leq x_{\text{max}}} \frac{\langle C_{2\text{pt}}(t_f) \text{Tr} [M^{-1}(\mathbf{x}, t; \mathbf{x}, t)] \rangle_c}{\langle C_{2\text{pt}}(t_f) \rangle}. \quad (37)$$

The subscript c (connected part) indicates that we subtract the product of the two individual vacuum expectation values from the numerator. Since no zero momentum projection is performed at the source of the two-point function, that resides at the spatial position $\mathbf{x} = \mathbf{0}$, the result will depend on the cut-off x_{max} . We expect the summand at large $|\mathbf{x}|$ to fall off exponentially in $|\mathbf{x}|$ so

TABLE I. The disconnected contribution to the scalar lattice matrix elements for different κ -combinations.

κ_{val}	κ_{cur}	V	$\langle N \bar{q}q N\rangle_{\text{dis}}^{\text{lat}}$
0.13550	0.13550	$32^3 64$	2.01(21)
		$40^3 64$	2.17(25)
	0.13609	$32^3 64$	2.27(22)
		$40^3 64$	2.43(27)
	0.13632	$32^3 64$	2.38(23)
		$40^3 64$	2.55(29)
0.13609	0.13550	$32^3 64$	1.97(20)
		$40^3 64$	2.06(25)
	0.13609	$32^3 64$	2.19(22)
		$40^3 64$	2.28(26)
	0.13632	$32^3 64$	2.21(23)
		$40^3 64$	2.36(28)
0.13632	0.13550	$32^3 64$	1.96(23)
		$40^3 64$	1.93(27)
	0.13609	$32^3 64$	2.06(24)
		$40^3 64$	2.05(29)
	0.13632	$32^3 64$	1.67(26)
		$40^3 64$	1.86(31)

that these values will eventually not contribute to the signal anymore but just increase the statistical noise. At very large spatial volumes one may therefore consider to perform such a partial sum only, thereby reducing the statistical error, and to estimate the induced bias by parameterizing the asymptotic fall-off.

We display the partial sums for the $L = 32a$ and $L = 40a$ lattices for the strangeness current at $\kappa_{\text{val}} = \kappa_{\text{sea}}$ in Fig. 5. We do not detect any statistically significant dependence of the curves on the value of t_f and show the results obtained at $t_f = 6a$. At small x_{max} we see the naively expected x_{max}^3 volume scaling. This becomes flatter around $x_{\text{max}} \approx 8a$ but only saturates to a constant once the boundary of the $L = 32a$ box is hit at $x_{\text{max}} = 16a$. Increasing x_{max} beyond this value means that in the case of this smaller lattice only the lattice “corners” are summed up. However, the $L = 40a$ data saturate at the same distance, rather than at $20a$, indicating that indeed the nucleon is well accommodated within this box size and that finite size effects are small.

C. Sea and valence quark contributions

The results of the bare disconnected scalar matrix elements for the two volumes (and three quark masses $m_q \leq m_s$) are displayed in Table I. For disconnected terms κ_{cur} can differ not only from κ_{sea} but also from the κ_{val} of the nucleon’s valence quarks. In Fig. 6 we display the dependence of the unrenormalized $f_{T_s}^{\text{lat}}$ -values on the

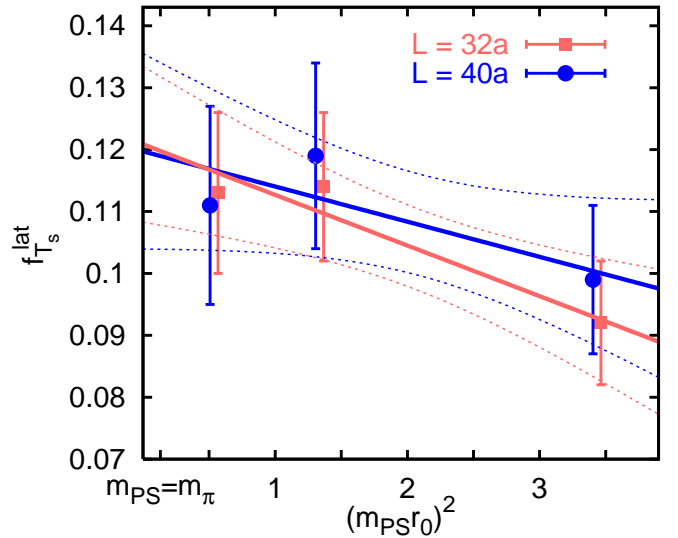


FIG. 6. The unrenormalized strange quark mass fraction $f_{T_s}^{\text{lat}}$, as a function of the valence pseudoscalar mass, for the two volumes.

valence quark mass of the proton for both volumes, together with linear chiral extrapolations. The right-most data points correspond to the strange quark mass and the left-most points to the present sea quark mass. The volume dependence is not significant and neither are the differences between the values obtained at the smallest mass point and the chirally extrapolated numbers. The results need to be renormalized and this is possible at $\kappa_{\text{val}} = \kappa_{\text{sea}} = 0.13632$.

To enable the calculation of the light σ -term and the renormalization of the strangeness matrix element, we also compute the connected contribution for $\kappa_{\text{cur}} = \kappa_{\text{val}} = \kappa_{\text{sea}} = 0.13632$, using the traditional sequential propagator method. We obtain $\langle N|\bar{u}u + \bar{d}d|N\rangle_{\text{con}}^{\text{lat}} = 8.43(73)$ and $8.35(43)$ for the $L = 32a$ and $L = 40a$ lattices, respectively. This means that at the pseudoscalar mass $m_{\text{PS}} \approx 285$ MeV the relative contribution of the disconnected matrix element reads

$$r^{\text{lat}} = \frac{\langle N|\bar{u}u + \bar{d}d|N\rangle_{\text{dis}}^{\text{lat}}}{\langle N|\bar{u}u + \bar{d}d|N\rangle^{\text{lat}}} = \begin{cases} 0.284(36) , & L = 32a \\ 0.308(37) , & L = 40a . \end{cases} \quad (38)$$

The unrenormalized values of Table I seem to be fairly independent of the current quark mass. The ratio of the strangeness matrix element over a light sea quark contribution undergoes the renormalization

$$\frac{2\langle \bar{s}s \rangle^{\text{ren}}}{\langle \bar{u}u + \bar{d}d \rangle_{\text{dis}}^{\text{ren}}} = \frac{2\langle \bar{s}s \rangle^{\text{lat}} - \frac{\alpha_Z}{1+\alpha_Z} \langle \bar{u}u + \bar{d}d \rangle^{\text{lat}}}{\langle \bar{u}u + \bar{d}d \rangle_{\text{dis}}^{\text{lat}} - \frac{\alpha_Z}{1+\alpha_Z} \langle \bar{u}u + \bar{d}d \rangle^{\text{lat}}} . \quad (39)$$

The renormalization of the numerator is obtained from Eq. (33) while the denominator can be split into two parts that renormalize with Z_m^s and with Z_m^{ns} , respectively: $\langle \bar{u}u + \bar{d}d \rangle - \langle \bar{u}u + \bar{d}d \rangle_{\text{con}}$. The $\text{SU}(3)_F$ flavour symmetry of the unrenormalized sea obviously cannot

disappear when subtracting the same (large) terms from the numerator and the denominator. However, this subtraction results in large statistical uncertainties. For instance on the large volume the above ratio reads 1.7 ± 5.5 with an additional systematic uncertainty of 0.5 from the value of the renormalization parameter α_Z , Eq. (29). We conclude that the renormalized sea is $SU(3)_F$ symmetric within a factor of about five.

The disconnected fraction r of Eq. (38) will undergo the renormalization

$$r^{\text{ren}} = (1 + \alpha_Z)r^{\text{lat}} - \alpha_Z = 0.024(5)^{+29}_{-9}. \quad (40)$$

The value quoted is obtained on the $L = 40a$ volume using the VWI prescription, with a systematic error that incorporates the difference between the two determinations of the renormalization constant ratios Eq. (29) and their respective uncertainties. For the renormalized y -parameter that is defined in Eq. (36) this implies that

$$y = r^{\text{ren}} \frac{2\langle \bar{s}s \rangle^{\text{ren}}}{\langle \bar{u}u + \bar{d}d \rangle_{\text{dis}}^{\text{ren}}} \approx r^{\text{ren}}, \quad (41)$$

where the approximation holds within a factor of five, see also Eq. (47) below.

D. The light and strange σ -terms

Combining all information results in the renormalized values for the pion-nucleon σ -term at the simulated sea quark mass

$$\sigma_{\text{PSN}} = \begin{cases} 0.0378(39)a^{-1} = 0.264(26)(2)r_0^{-1}, & L = 32a \\ 0.0389(36)a^{-1} = 0.272(25)(2)r_0^{-1}, & L = 40a \end{cases} \quad (42)$$

at the two different volumes, where the second error is due to the uncertainty of the chirally extrapolated r_0 -value. The above σ -term can also be obtained from the derivative of the nucleon mass with respect to the logarithm of the light quark mass. Using the fact that at small m_{PS} , $m_u + m_d \propto m_{\text{PS}}^2$, we can write

$$\sigma_{\text{PSN}} = m_u \frac{\partial m_N}{\partial m_u} + m_d \frac{\partial m_N}{\partial m_d} \approx m_{\text{PS}}^2 \frac{dm_N}{dm_{\text{PS}}^2}. \quad (43)$$

To leading order in chiral perturbation theory $dm_N/dm_{\text{PS}}^2 = \text{const.}$ This linear assumption suggests to multiply the result Eq. (42) with the ratio $m_{\pi, \text{phys}}^2/m_{\text{PS}}^2$ to obtain the physical σ -term $\sigma_{\pi N}^{\text{phys},0} = 0.064(6)r_0^{-1} = 25(3)(1) \text{ MeV}$. In general, however, higher order corrections will lead to some curvature.

Fortunately, we do not only know the σ -term at $\kappa = 0.13632$ but also the nucleon mass [22] at other values of $\kappa_{\text{val}} = \kappa_{\text{sea}}$, at $\beta = 5.29$ ($a^{-1} \approx 2.71 \text{ GeV}$) and at $\beta = 5.4$ ($a^{-1} \approx 3.22 \text{ GeV}$), see Table II. A combined $\mathcal{O}(p^4)$ covariant $B\chi\text{PT}$ [34] fit to these data within the window

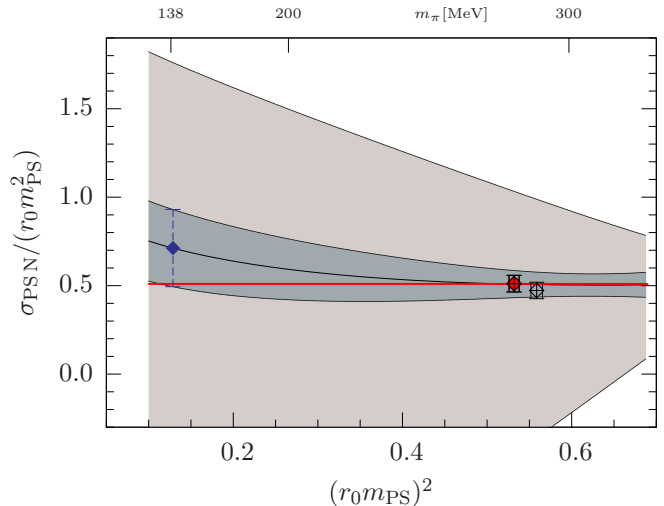


FIG. 7. Extrapolation of $\sigma_{\text{PSN}}/m_{\text{PS}}^2$ to the physical point [22] using covariant $B\chi\text{PT}$. The open symbols correspond to the values that we directly obtain at $m_{\text{PS}}r_0 \approx 0.73$ on the $L = 40a$ volume (left) and for $L = 32a$ (right). The broad error band is obtained when ignoring this constraint. The horizontal line denotes the (constant) leading order expectation.

TABLE II. QCDSF pseudoscalar and nucleon masses [22] at $\beta = 5.29$ ($a^{-1} \approx 2.7 \text{ GeV}$) and $\beta = 5.40$ ($a^{-1} \approx 3.2 \text{ GeV}$).

β	κ	V	am_{PS}	am_N	$r_0 m_{\text{PS}}$	$r_0 M_N$
5.29	0.13620	$24^3 48$	0.1552(6)	0.467(5)	1.084(9)	3.26(4)
5.29	0.13632	$24^3 48$	0.1112(9)	0.425(6)	0.776(8)	2.97(5)
5.29	0.13632	$32^3 64$	0.1070(4)	0.390(5)	0.747(6)	2.72(4)
5.29	0.13632	$40^3 64$	0.1050(3)	0.381(3)	0.733(6)	2.66(3)
5.40	0.13660	$32^3 64$	0.0845(6)	0.353(7)	0.700(8)	2.92(7)
5.40	0.13660	$48^3 64$	0.0797(3)	0.314(5)	0.660(7)	2.60(5)

$250 \text{ MeV} < m_{\text{PS}} < 430 \text{ MeV}$, imposing our directly obtained value of σ_{PSN} as an additional constraint, results in the preliminary number [22]

$$\sigma_{\pi N}^{\text{phys}} = (38 \pm 12) \text{ MeV} \quad (44)$$

at the physical point. The error includes both the statistical uncertainty of the fit and the systematics from varying the low energy parameters c_2 , c_3 and l_3 within their phenomenologically allowed ranges [34–36]. A detailed analysis will be presented in Ref. [22]. We display the result of this extrapolation in Fig. 7 for the ratio $\sigma_{\text{PSN}}/m_{\text{PS}}^2$ in units of r_0 , together with our direct determinations. The broad error band indicates the result of the same fit, without using our constraint at $m_{\text{PS}} \approx 285 \text{ MeV}$.

We now use Eq. (35) with α_Z given in Eq. (29) to obtain the renormalized strangeness matrix element from the values given above. This amounts to subtracting numbers of similar sizes from each other. There is no noticeable finite size effect between the 32^3 and 40^3 vol-

umes. For our simulation point at a low pion mass $m_{\text{PS}} \approx 285$ MeV we obtain the values, $a[m_s \langle N | \bar{s}s | N \rangle]^{\text{ren}} = 0.005(6)$ and $0.008(6)$ for the two determinations of the renormalization parameter α_Z from the VWI and AWI, respectively.

Of particular phenomenological interest is the dimensionless strange quark contribution to the nucleon mass

$$f_{T_s} = \frac{[m_s \langle N | \bar{s}s | N \rangle]^{\text{ren}}}{m_N} = 0.012(14)_{-3}^{+10}. \quad (45)$$

Again, we quote the value obtained from the VWI prescription, with a systematic error that incorporates the difference between the two determinations of the renormalization constant ratios and their respective uncertainties. This may be indicative of $\mathcal{O}(a)$ effects. The problem of large cancellations cannot be overcome easily. One needs to get closer to the continuum limit so that α_Z approaches zero. For instance, at $\beta = 5.40$, $\alpha_Z \approx 0.2$ [29], significantly reducing the subtraction of the connected diagram (and probably the value of $\langle N | \bar{s}s | N \rangle^{\text{lat}}$ that will contain a smaller light quark contribution).

The result obtained is interesting insofar as it suggests a scalar strangeness of less than 4 % of the nucleon mass, $\sigma_s = 12_{-16}^{+23}$ MeV. In spite of the relative enhancement by the ratio $m_s/m_{ud} > 25$ this is not bigger than the pion-nucleon σ -term above. This is quite consistent with the finding of Eq. (40) of a tiny renormalized light sea quark participation in σ_{PSN} . We remark that taking the combination $m_s^{\text{lat}} \langle N | \bar{s}s | N \rangle^{\text{lat}}$ without the proper subtraction would have resulted in $f_{T_s} \approx 0.12$, even bigger than the light quark mass contribution of about 0.09, at our light quark mass value that exceeds the physical one by a factor of about four. Neglecting the mixing with light quarks in the renormalization is probably the main reason why this contribution was overestimated in the pioneering lattice studies, see e.g. Ref. [37] and references therein. Early results are also summarized in Ref. [19]

We can constrain the scale-independent y -ratio of Eq. (36),

$$y = \begin{cases} (1 + \alpha_Z) 0.333(36) - \alpha_Z, & L = 32a \\ (1 + \alpha_Z) 0.320(33) - \alpha_Z, & L = 40a \end{cases} \quad (46)$$

$$= \begin{cases} 0.059(37)(28), & L = 32a \\ 0.041(37)(29), & L = 40a, \end{cases} \quad (47)$$

where the errors are statistical and the difference between the two determinations of α_Z , respectively. Again, as the central value, we have taken the result from the VWI renormalization factor. From our determination of the pion-nucleon σ -term we know that the denominator of Eq. (36) will increase by a factor 1.4–1.5 when extrapolated to the chiral limit. Based on the weak observed dependence of $\langle N | \bar{s}s | N \rangle^{\text{lat}}$ on the valence quark mass, see Fig. 6, we would expect the numerator to exhibit a less pronounced quark mass dependence. Thus a 95 % confidence-level upper limit on the y -parameter $y < 0.14$ should also apply at physically light sea quark masses.

Finally, we also predict the gluonic and heavy sea quark contribution f_{T_G} of Eq. (4),

$$f_{T_G} = 1 - \frac{\sigma_{\pi N} + \sigma_s}{m_N} = 0.951_{-27}^{+20}. \quad (48)$$

This means that the light and strange quark flavours contribute a fraction between 3 % and 8 % to the nucleon mass.

V. SUMMARY

We directly calculate the light quark and strangeness σ -terms on lattices with spatial extents up to $Lm_{\text{PS}} \approx 4.2$, a lattice spacing $a^{-1} \approx 2.71$ GeV and a pseudoscalar mass $m_{\text{PS}} \approx 285$ MeV. At this mass point and lattice spacing the quark line disconnected contribution amounts to a fraction of $r^{\text{lat}} \approx 0.3$ of the full result. After renormalization however we find this number to drop below the 5 % level, see Eq. (40).

At our fixed mass point we obtain the renormalized values, $\sigma_s = 12_{-16}^{+23}$ MeV and $\sigma_{\text{PSN}} = 106(11)(3)$ MeV, for the strangeness and light quark σ -terms. Assuming the latter value to depend linearly on m_{PS}^2 , as predicted by leading order chiral perturbation theory, this corresponds to $25(3)$ MeV at the physical point. However, from nucleon mass data obtained at pseudoscalar masses, $250 \text{ MeV} < m_{\text{PS}} < 430 \text{ MeV}$, it is clear that there exists a non-vanishing curvature. Our direct determination can be used to strongly constrain an $\mathcal{O}(p^4)$ covariant baryon chiral perturbation theory extrapolation of the nucleon mass [22]. The combined fit yields the preliminary value $\sigma_{\pi N}^{\text{phys}} = (38 \pm 12)$ MeV at the physical point. Without the direct information on the slope at one point the statistical and systematic uncertainties would have been much larger, see Fig. 7. It would be difficult to significantly reduce this large error, without nucleon mass data at physical and, possibly, smaller than physical quark masses.

We are also able to exclude values $y > 0.14$ of the y -parameter, with a confidence level of 95 %. This means that the strangeness contribution to the scalar coupling of the nucleon is much smaller than that due to the light quark σ -term. To determine the strangeness σ -term using the indirect method, i.e. the Feynman-Hellmann theorem, requires $n_F = 2 + 1$ sea quark flavours. Even then the dependence of the nucleon mass on the strange quark mass will be very weak and the tiny slope (and its error) will be amplified by the mass ratio $m_s/m_{ud} > 25$. Therefore, for an accurate prediction of f_{T_s} , and in particular for a non-vanishing lower bound on its value, an additional direct determination at one or a few mass points will be crucial.

We remark that the results presented here have not been extrapolated to the continuum limit. Neither has the effect of quenching the strange quark been addressed, except within the renormalization of the strangeness σ -term.

ACKNOWLEDGMENTS

We thank Peter Bruns and Ludwig Greil for discussion. This work was supported by the European Union under Grant Agreement number 238353 (ITN STRONGnet) and by the Deutsche Forschungsgemeinschaft SFB/Transregio 55. Sara Collins acknowledges support from the Claussen-Simon-Foundation (Stifterverband für die Deutsche Wissenschaft). André Sternbeck was supported by the EU International Reintegration Grant (IRG) 256594. James Zanotti was sup-

ported by the Australian Research Council under grant FT100100005 and previously by the Science & Technology Facilities Council under grant ST/F009658/1. Computations were performed on the SFB/TR55 QPACE supercomputers, the BlueGene/P (JuGene) and the Nehalem Cluster (JuRoPA) of the Jülich Supercomputer Center, the IBM BlueGene/L at the EPCC (Edinburgh), the SGI Altix ICE machines at HLRN (Berlin/Hannover) and Regensburg's Athene HPC cluster. We thank the support staffs of these institutions. The Chroma software suite [38] was used extensively in this work and gauge configurations were generated using the BQCD code [39] on QPACE and BlueGenes.

-
- [1] J. Ellis, K. A. Olive and P. Sandick, *New J. Phys.* **11**, 105015 (2009) [arXiv:0905.0107 [hep-ph]].
 - [2] M. A. Shifman, A. I. Vainshtein and V. I. Zakharov, *Phys. Lett. B* **78**, 443 (1978).
 - [3] A. Kryjevski, *Phys. Rev. D* **70**, 094028 (2004) [arXiv:hep-ph/0312196].
 - [4] G. Aad *et al.* [ATLAS Collaboration], arXiv:0901.0512 [hep-ex].
 - [5] J. Gasser, H. Leutwyler and M. E. Sainio, *Phys. Lett. B* **253**, 252 (1991).
 - [6] M. M. Pavan, I. I. Strakovsky, R. L. Workman and R. A. Arndt, *PiN Newsl.* **16**, 110 (2002) [arXiv:hep-ph/0111066].
 - [7] B. Borasoy and U.-G. Meissner, *Phys. Lett. B* **365**, 285 (1996) [arXiv:hep-ph/9508354].
 - [8] J. M. Alarcón, J. Martin Camalich and J. A. Oller, arXiv:1110.3797 [hep-ph].
 - [9] R. Babich, R. C. Brower, M. A. Clark, G. T. Fleming, J. C. Osborn, C. Rebbi and D. Schaich, arXiv:1012.0562 [hep-lat].
 - [10] T. Doi *et al.* [χ QCD Collaboration], *AIP Conf. Proc.* **1374**, 598 (2011) [arXiv:1010.2834 [hep-lat]]; T. Doi *et al.* [χ QCD Collaboration], *Phys. Rev. D* **80**, 094503 (2009) [arXiv:0903.3232 [hep-ph]].
 - [11] C. Alexandrou, K. Hadjiyiannakou, G. Koutsou, A. Ó Cais and A. Strelchenko, arXiv:1108.2473 [hep-lat].
 - [12] M. Engelhardt, *PoS LATTICE2010*, 137 (2010) [arXiv:1011.6058 [hep-lat]].
 - [13] K. Takeda, S. Aoki, S. Hashimoto, T. Kaneko, J. Noaki and T. Onogi [JLQCD Collaboration], *Phys. Rev. D* **83**, 114506 (2011) [arXiv:1011.1964 [hep-lat]].
 - [14] S. Dürr *et al.*, *Phys. Rev. D* **85**, 014509 (2012) [arXiv:1109.4265 [hep-lat]]; *PoS LATTICE2010*, 102 (2010) [arXiv:1012.1208 [hep-lat]].
 - [15] R. Horsley *et al.* [QCDSF and UKQCD Collaborations], *Phys. Rev. D* **85**, 034506 (2012) [arXiv:1110.4971 [hep-lat]].
 - [16] R. Horsley *et al.* [QCDSF and UKQCD Collaborations], *Phys. Rev. D* **83**, 051501 (2011) [arXiv:1012.0215 [hep-lat]].
 - [17] D. Toussaint and W. Freeman [MILC Collaboration], *Phys. Rev. Lett.* **103**, 122002 (2009) [arXiv:0905.2432 [hep-lat]].
 - [18] R. D. Young and A. W. Thomas, *Phys. Rev. D* **81**, 014503 (2010) [arXiv:0901.3310 [hep-lat]].
 - [19] R. D. Young and A. W. Thomas, *Nucl. Phys. A* **844**, 266C (2010) [arXiv:0911.1757 [hep-lat]].
 - [20] G. S. Bali, S. Collins and A. Schäfer [QCDSF Collaboration], *PoS LAT2009*, 149 (2009) [arXiv:0911.2407 [hep-lat]].
 - [21] S. Collins, G. S. Bali, A. Nobile, A. Schäfer, Y. Nakamura and J. Zanotti [QCDSF Collaboration], *PoS LATTICE2010*, 134 (2010) [arXiv:1011.2194 [hep-lat]].
 - [22] G. Schierholz, A. Sternbeck *et al.* [QCDSF Collaboration], in preparation.
 - [23] J. Najjar *et al.* [QCDSF Collaboration], in preparation.
 - [24] G. S. Bali, H. Neff, T. Düssel, T. Lippert and K. Schilling [SESAM Collaboration], *Phys. Rev. D* **71**, 114513 (2005) [arXiv:hep-lat/0505012].
 - [25] S. Güsken *et al.*, *Phys. Lett. B* **B227**, 266 (1989); S. Güsken, *Nucl. Phys. B Proc. Suppl.* **17**, 361 (1990).
 - [26] M. Falcioni, M. L. Paciello, G. Parisi and B. Taglienti, *Nucl. Phys. B* **251**, 624 (1985).
 - [27] S. Bernardson, P. McCarty and C. Thron, *Comput. Phys. Commun.* **78**, 256 (1994).
 - [28] G. S. Bali, S. Collins and A. Schäfer, *Comput. Phys. Commun.* **181**, 1570 (2010) [arXiv:0910.3970 [hep-lat]].
 - [29] M. Göckeler *et al.* [QCDSF and UKQCD Collaborations], *Phys. Lett. B* **639**, 307 (2006) [arXiv:hep-ph/0409312]; P. E. L. Rakow, *Nucl. Phys. Proc. Suppl.* **140**, 34 (2005) [arXiv:hep-lat/0411036] and private notes.
 - [30] T. Bhattacharya and R. Gupta, *Nucl. Phys. B Proc. Suppl.* **63**, 95 (1998) [arXiv:hep-lat/9710095].
 - [31] T. Bhattacharya, R. Gupta, W. Lee, S. R. Sharpe and J. M. S. Wu, *Phys. Rev. D* **73**, 034504 (2006) [arXiv:hep-lat/0511014].
 - [32] C. Michael, C. McNeile and D. Hepburn [UKQCD Collaboration], *Nucl. Phys. B Proc. Suppl.* **106**, 293 (2002) [arXiv:hep-lat/0109028].
 - [33] M. Göckeler *et al.* [QCDSF Collaboration], *Phys. Rev. D* **82**, 114511 (2010) [arXiv:1003.5756 [hep-lat]] and reanalysis by M. Göckeler, private communication.
 - [34] T. Becher and H. Leutwyler, *JHEP* **0106**, 017 (2001) [arXiv:hep-ph/0103263].
 - [35] M. Frink and U.-G. Meissner, *JHEP* **0407**, 028 (2004) [arXiv:hep-lat/0404018].
 - [36] G. Colangelo *et al.* [FLAG Working Group], *Eur. Phys. J. C* **71**, 1695 (2011) [arXiv:1011.4408 [hep-lat]]; <http://itpwiki.unibe.ch/flag/>.
 - [37] S. Güsken, arXiv:hep-lat/9906034.

- [38] R. G. Edwards and B. Joó [SciDAC, LHP and UKQCD Collaborations], Nucl. Phys. Proc. Suppl. **140**, 832 (2005) [arXiv:hep-lat/0409003];
C. McClendon, Jlab preprint JLAB-THY-01-29 (2001);
P. A. Boyle, Comput. Phys. Commun. **180**, 2739 (2009).
- [39] Y. Nakamura and H. Stüben, PoS **LATTICE2010**, 040 (2010) [arXiv:1011.0199 [hep-lat]].